Anisotropy of core-level photoemission from InSe, GaSe, and cesiated W(001)

N. V. Smith, P. K. Larsen,* and S. Chiang†
Bell Laboratories, Murray Hill, New Jersey 07974
(Received 8 June 1977)

The angular dependence of photoemission from the In 4*d* and Ga 3*d* core levels in the layer compounds InSe and GaSe has been measured. Azimuthal anisotropies are found to be quite strong. Asymmetries associated with the strong polarization of the synchrotron radiation source are discussed, and it is shown that more information is obtained with an analyzer sampling photoelectrons propagating out of the plane of incidence rather than in it. Similar measurements of the 5*p* core levels of Cs adsorbed on the (001) face of W show some indications of anisotropy at low coverages. The relevance of these results to the proposed use of photoelectron diffraction for surface-structure determination is discussed.

I. INTRODUCTION

Angle-resolved photoemission is a fairly recent refinement of the photoemission technique, and is attracting a considerable amount of experimental and theoretical attention. With few exceptions,[1-4] most experiments so far have concentrated on the emission from valence levels. A more tractable problem theoretically, however, is the emission from a localized core level. One does not then have to contend with a band-structure problem for both the initial- and final-state wave functions in the optical transition. Rather, one is able to isolate the diffraction effects experienced by the photoelectron in its final state.

We present, in this paper, experimental results for the angular dependence of photoemission from the In 4*d* and Ga 3*d* core levels in the layer materials InSe and GaSe, respectively. We show that the form of the results depends primarily on the final-state energy. We report significant effects due to the strong polarization of the synchrotron radiation source used in these measurements, and we indicate the nature of the additional information obtained.

By way of contrast we report also some results obtained on the angular dependence of photoemission from the Cs 5*p* core levels for Cs atoms adsorbed on the (001) face of single-crystal W. As discussed in Sec. II, emission from adsorbed Cs represents a backscattering configuration, whereas emission from In and Ga atoms in their respective selenides represents a forward-scattering configuration. The results and comparisons are of relevance to the feasibility of recent proposals to use angle-resolved core-level photoemission as a kind of low-energy-electron diffraction (LEED) technique.

II. THEORETICAL PERSPECTIVE

The theory of the angular dependence of photoemission from an adsorbate core level has been expounded by a number of authors.[5-7] According to Liebsch,[5] whose formalism and nomenclature we will adopt from hereon, the wave function at the position $\vec{R}$ of the detector of an outgoing photoelectron emitted from an atom at the origin is written

$$\Psi(\vec{R}) = \int d^3r\, G(\vec{R},\vec{r})\vec{p}\cdot\vec{A}\Psi_i(\vec{r}) \equiv G\vec{p}\cdot\vec{A}\,|\Psi_i\rangle\,, \tag{1}$$

where Ψ_i is the initial-core-state wave function and G is the final-state one-electron propagator for the motion of the photoelectron in the full potential due to the substrate and adsorbed atoms. The wave function of Eq. (1) can be expressed as two contributions

$$\Psi(\vec{R}) = \Psi^0(\vec{R}) + \Psi^1(\vec{R})\,. \tag{2}$$

The first represents the intra-atomic or central-site contribution, and is given by

$$\Psi^0(\vec{R}) \equiv (G_0 + G_0 t_0 G_0)\vec{p}\cdot\vec{A}\,|\Psi_i\rangle\,, \tag{3}$$

where G_0 is the electron propagator in the absence of the lattice potential and t_0 represents a single-site scattering vertex. The second contribution accounts for the presence of the surrounding atoms and is given by

$$\Psi^1(\vec{R}) \equiv G_0 T'\,|\Psi^0\rangle\,, \tag{4}$$

where T' is the remaining part of the T matrix for the entire system after the central-site interaction has been separated out.

The physics of this formal separation is represented pictorially in Fig. 1. The contribution Ψ^0 is termed the "direct" wave and is represented by a full line propagating directly towards the detector. The contribution Ψ^1 is termed the "indirect" contribution and consists of processes such as those represented by the dashed lines in Fig. 1. Both single- and multiple-scattering processes are contained within Ψ^1. It is the interference of

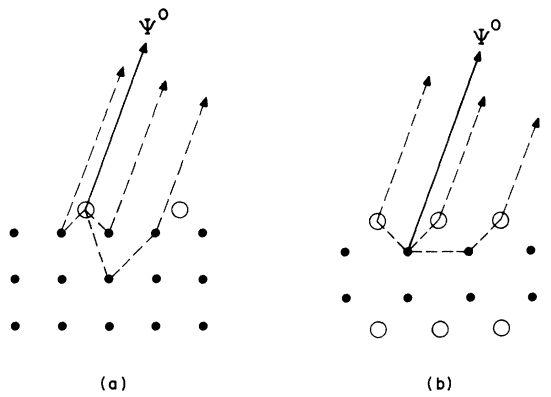

FIG. 1. Schematic representation of the scattering geometry for core-level photoemission from (a) an adsorbed Cs atom on the W(001) surface; (b) an In atom within a sandwich of the layer compound InSe. The full arrows represent the direct wave Ψ^0; dashed arrows correspond to scattered contributions.

these processes with each other and with Ψ^0 which gives rise to the observed anisotropies in the photoemission. Viewed from this point of view, angle-resolved photoemission from core levels is seen as a kind of LEED experiment which could, in principle, be used to determine adsorbate positions. Indeed, the need to test the feasibility of such a technique was the main motivation for the experimental work reported in this paper. Such a technique, which might appropriately be termed photoelectron diffraction, has potential advantages over LEED. Firstly, by using the energy-resolving capability of photoemission, one can tune in on surface-atom core levels and thereby arrange that one's entire signal is coming from the very atoms whose position one is trying to determine. Secondly, the adsorbate overlayer does not have to be periodic, as in LEED.

Figure 1 shows in a highly schematic fashion the atomic arrangement in the two systems we have studied experimentally. Fig. 1(a) shows Cs atoms (large open circles) adsorbed on the (001) face of W (atoms represented by small full circles). The $5p$ core levels of Cs are quite accessible, having energies in the range -15 to -11 eV with respect to the Fermi level. This system is very close in spirit to the systems envisaged by Liebsch in his original papers, i.e., the indirect terms (at least for low coverages) correspond to backscattering from the substrate. The other systems we have chosen for study are the compounds InSe and GaSe; the atomic arrangement is shown schematically in Fig. 1(b). The crystal consists of layers in which two sheets of In or Ga atoms (small full circles) are "sandwiched" between two sheets of Se atoms (large open circles). The crystals cleave between sandwiches, so that the outermost, or surface, sheet is composed of Se atoms. The In and Ga atoms have accessible core levels, namely, the $4d$ states of In and the $3d$ states of Ga. Note that photoelectrons generated on the In or Ga atoms must all pass through the surface sheet of Se atoms in order to reach the detector. This therefore represents a forward-scattering situation which, it was thought, should provide an instructive contrast with the backscattering situation of Cs on W(001).

Let us now consider the form of Ψ^0 in relation to the particular experimental geometry we have chosen. Ψ^0 is the quantity which would determine the angular dependence of the photoemission cross section in the gas phase. [In the approximation where the $G_0 t_0 G_0$ term of Eq. (3) is neglected, Ψ^0 is simply a plane wave, and one retrieves the familiar theorem in which the angular dependence of the photoemission intensity replicates the angular dependence of the initial-state atomic orbital.[8]] In our experimental arrangement, the azimuthal angle ϕ is varied by rotating the *sample* rather than moving the *detector*. If the sample were to consist of an assembly of weakly interacting (i.e. essentially isolated) atoms the intensity of the core-level emission would not vary as the sample is rotated since there is no preferred direction within the sample against which to relate the atomic orbitals. If any variations with ϕ are observed, they can be due only to the existence of a nonzero Ψ^1 term. Our choice of experimental geometry, therefore, permits us to isolate and study the final-state scattering, or photoelectron-diffraction effects, represented by Ψ^1.

Finally, we point out that the intensity measured at the detector is of the form $|\vec{A}\cdot\vec{M}|^2$, where $\vec{M}$ is some generalized one-step matrix element for the photoemission process. A similar factor, however, would appear also in any expression for the photoemission intensity using a three-step model for the photoemission process. In that case, $\vec{M}$ would be the momentum matrix element for step one, the optical excitation. In either case $\vec{M}$ must embody the symmetry of the crystal or surface under study. In Sec. IV, we will discuss how the interplay between crystal symmetry and the $|\vec{A}\cdot\vec{M}|^2$ form for the photoemission probability affects the observed phenomenology.

III. EXPERIMENTAL DETAILS

A. Measuring system

The experiments were performed in a two-analyzer system which has been described elsewhere.[9] The system uses synchrotron radiation from the Tantalus I storage ring located at the University of Wisconsin Physical Sciences Laboratory, Stough-

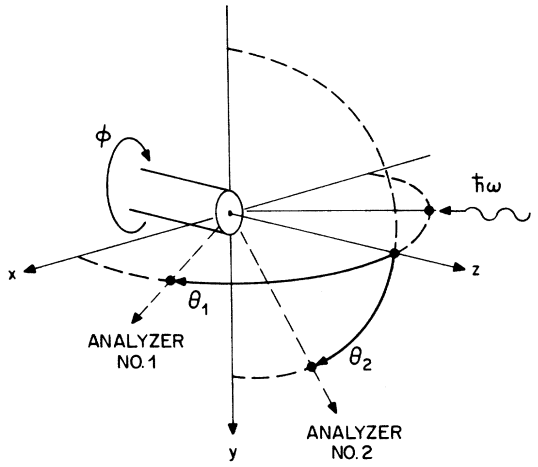

FIG. 2. Geometry of the experimental setup, defining the x, y, z axes and the angular degrees of freedom.

ton, Wisc. The radiation was monochromatized by a newly installed ultrahigh-vacuum vertically dispersing Seya-Namioka monochromator. The geometry of the setup is illustrated in Fig. 2. The radiation is incident at 45° in the horizontal xz plane. This plane contains the normal to the sample surface (z axis) and the polarization vector $\vec{A}$ of the synchrotron radiation. The system is equipped with two electron energy analyzers of the plane mirror type. Analyzer No. 1 samples photoelectrons in the horizontal plane and can be set at various polar angles θ_1 with respect to the surface normal. Analyzer No. 2 samples photoelectrons in the vertical yz plane and can be set at polar angles θ_2 with respect to the surface normal. The other angular degree of freedom is ϕ, the azimuthal angle or angle of rotation of the sample about the surface normal. The base pressure of the system, even while open to the monochromator and storage ring, is $\sim 2 \times 10^{-10}$ Torr.

B. Sample preparation

Clean surfaces of the layer compounds InSe and GaSe were prepared by cleavage in the ultrahigh-vacuum chamber. The cleaving procedure is described elsewhere.[10] These materials are relatively inert, and the surfaces thus prepared last for the several days required to perform the experiments without serious deterioration. The core-level measurements described here were performed subsequent to the valence-band measurements reported earlier.[11,12]

The single-crystal samples of W(001) were prepared and cleaned by standard techniques. The crystals were heated resistively in an oxygen atmosphere (10^{-7} Torr) at relatively low temperatures (1000 °C) to remove carbon from the surface region, and were subsequently flashed at high temperatures (~2400°C) *in vacuo* just prior to actual measurements. Results obtained for the angular dependence of photoemission from these clean W(001) samples were essentially identical to those obtained by others.[13,14] In particular, we observed the prominent surface state from just below the Fermi level and monitored its angular dependence. These results will not be described in any further detail.

Cesium was applied to the W(001) samples by evaporation from commercially available Cs sources. Two sources were used, one to cover the front face of the sample, the other to cover the back face and supporting fixtures. Uniformity of coverage is important because of the large changes in work function on exposure to Cs. Differences in work function between the front and back surfaces of the sample give rise to fringing electrostatic fields which can seriously distort the trajectories of photoemitted electrons. It is at low coverages (less than $\frac{1}{4}$ monolayer) where the work function is changing rapidly that this problem is most severe.

C. Procedure and data manipulation

Some typical spectra obtained on InSe and GaSe in the core-level region are shown in Fig. 3. In

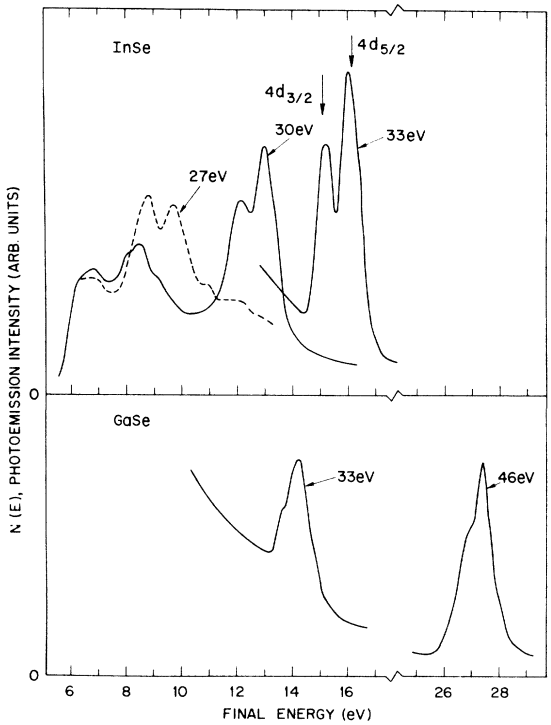

FIG. 3. Typical photoelectron energy spectra at various photon energies, taken in the core-level region on InSe and GaSe.

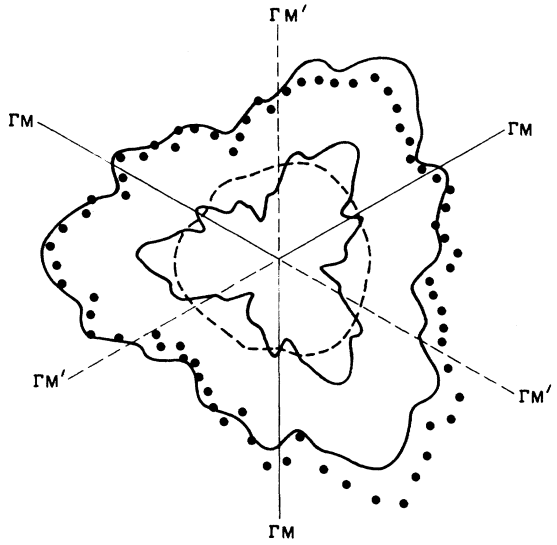

FIG. 4. Radial plot of the azimuthal dependence of the 3*d* core-level photoemission intensity in GaSe, taken with analyzer No. 2 at $\theta_2 = 65°$ at $\hbar\omega = 33$ eV. Full circles represent the raw data. The smooth curves involve threefold averaging and are explained in the text.

the case of InSe it is seen that the In 4*d* core level is spin-orbit split into $4d_{3/2}$ and $4d_{5/2}$ components separated by 0.9 eV. For the Ga 3*d* levels in GaSe the spin-orbit splitting of 0.4 eV is less well resolved. Spectra were recorded as a function of polar angle at constant photon energy to determine whether there was any dispersion in energy of the core levels; however, no significant dispersion was found.

The azimuthal dependence of the core-level emission was determined by selecting the proper final-state energy corresponding to the chosen photon energy and measuring the photoelectron intensity when the sample is rotated about its normal. Figure 4 shows a radial plot of the azimuthal intensity for the Ga 3*d* core level at $\hbar\omega = 33$ eV obtained with analyzer No. 2 at $\theta_2 = 65°$. The full circles represent the raw data. The outer full curve is a symmetrized version of the data which exploits the known threefold rotational symmetry of the sample; it is a smooth curve drawn through the symmetrized data points $I'(\phi)$ given by

$$I'(\phi) \equiv [I(\phi) + I(\phi + \tfrac{2}{3}\pi) + \tfrac{1}{3} I(\phi - \tfrac{2}{3}\pi)]. \quad (5)$$

We point out that the structures in the symmetrized curve $I'(\phi)$ are reproducible in the sense that they repeat every 120°. The deviations between the raw data points, $I(\phi)$, and the threefold symmetrized curve, $I'(\phi)$, are attributed to a slight wobbling and "walking" of the illuminated spot over the surface as the sample is rotated.

The spectra of Fig. 3 show that the core-level emission is superposed on a background signal which is attributed to inelastically scattered electrons. A linear background subtraction procedure was applied to the data to isolate the true core-level emission. This consisted of measuring the azimuthal dependence at energies just above and just below the core-level peak and then making a linear interpolation. The threefold symmetrized version of this background signal is shown as the dashed curve in Fig. 4, and it is seen to be very close to constant. The inner full curve of Fig. 4 shows the Ga 3*d* core-level emission after this background signal has been removed. The azimuthal plots shown in the remainder of this paper have had a background subtracted and have been symmetrized in the manner indicated above. In the case of the W(001) experiments we use, of course, a fourfold rather than threefold symmetrizing procedure. Since we will be concerned below with mirror symmetries in the azimuthal patterns, it is important to point out that these mirror symmetries are not produced artificially by the rotational symmetrizing procedures just described.

IV. RESULTS AND DISCUSSION ON InSe AND GaSe

Results obtained at $\hbar\omega = 33.0$ eV for the azimuthal dependence of photoemission from the In 4*d* levels in InSe are shown in Fig. 5. Full curves were obtained with analyzer No. 1 ($\theta_1 = 60°$), and the dashed curves were obtained with analyzer No. 2 ($\theta_2 = 60°$). Figures 5(a) and 5(b) correspond to the $4d_{3/2}$ and $4d_{5/2}$ levels, respectively. We note, firstly, that the azimuthal anisotropies are quite strong, and, secondly, that there are significant differences between cases (a) and (b).

In Fig. 5(c), we show the azimuthal dependence at the same polar angles for the In $4d_{3/2}$ at $\hbar\omega = 33.9$. In this measurement the photon energy has been shifted deliberately by 0.9 eV in order to deposit the photoelectrons at the same final-state energy as for the $4d_{5/2}$ level at $\hbar\omega = 33.0$ eV. The form of Fig. 5(c) bears a stronger resemblance to that of Fig. 5(b) rather than Fig. 5(c) indicating that the results depend primarily on the final-state energy.

An interesting feature of the results of Fig. 5 is that the azimuthal patterns obtained with the out-of-plane analyzer do not display the mirror symmetry about the Γ*M* azimuths possessed by the crystal itself. (For a definition of the Γ*M* direction and other properties of the Brillouin zone, see Refs. 10 and 11.) The explanation of this effect was pointed out to us by Traum[15] and arises through an interference effect between components of the momentum matrix element $\vec{M}$ perpendicular and parallel to the crystal surface. Taking the x,

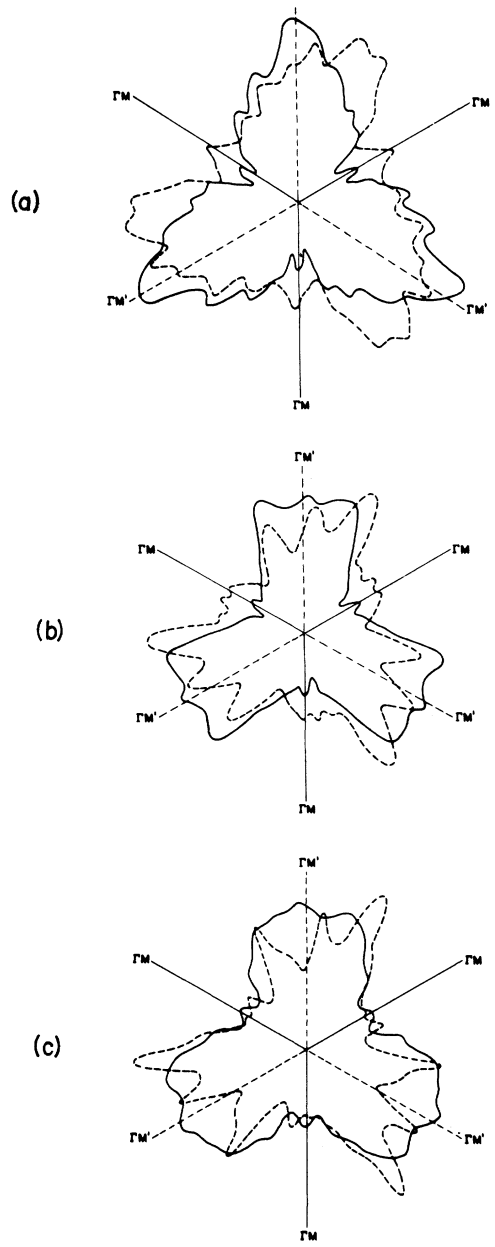

FIG. 5. Azimuthal dependence of the In $4d$ photoemission from InSe. Full (dashed) curves were obtained with analyzer No. 1 (No. 2) at the polar angle 60°. (a) $4d_{3/2}$ level at $\hbar\omega = 33$ eV; (b) In $4d_{5/2}$ level at $\hbar\omega = 33$ eV; (c) In $4d_{3/2}$ level at $\hbar\omega = 33.9$ eV.

y, and z axes as indicated in Fig. 2, and noting that the synchrotron radiation is horizontally polarized, we have $A_y = 0$. We also have $A_x = \beta A_z$, where β is determined by the optical constants of the solid. There are possible effects due to the strong variations of A_z in the surface region,[16] but these are not discussed explicitly here, since they do not affect the outcome of our argument. The expression for the azimuthal dependence of the photoemission intensity is

$$I(\phi) = cA_z^2 |\beta M_x(\phi) + M_z(\phi)|^2 , \tag{6}$$

where c is a constant. Let us now consider what happens as two azimuths which are equivalent to each other by mirror symmetry are rotated alternately into "line of sight" of the two analyzers. It is useful here to introduce a semipolar coordinate system (r, ϕ, z) fixed with respect to the crystal surface. With $\hat{r}$ denoting the radial unit vector and $\hat{t}$ a cross unit vector perpendicular to $\hat{r}$ in the xy plane, we can write,

$$\vec{M}(\phi) = M_r(\phi)\hat{r} + M_t(\phi)\hat{t} + M_z(\phi)\hat{z} . \tag{7}$$

If the zero of the azimuth ϕ is defined along a particular ΓM azimuth in the crystal surface, symmetry considerations give

$$\begin{aligned} M_r(-\phi) &= M_r(\phi) , \\ M_t(-\phi) &= -M_t(\phi) , \\ M_z(-\phi) &= M_z(\phi) . \end{aligned} \tag{8}$$

Analyzer No. 2 samples the yz plane, for which we have $M_x = M_t$. In Eq.(6), M_x can therefore change sign, while M_z, on the other hand, will be unchanged. Depending on the sign of M_x the interference between M_x and M_z will be constructive or destructive. This accounts qualitatively for the observed asymmetry of the azimuthal rotation patterns obtained with analyzer No. 2. Analyzer No. 1 samples the zx plane and $M_x = M_r$. Both M_r and M_z remain unchanged for a change in sign of ϕ and mirror symmetry will be preserved as is actually observed in the full curves of Fig. 5.

These effects can be examined more quantitatively by forming appropriate symmetric and antisymmetric combinations. For analyzer No. 2,

$$\begin{aligned} I^+(\phi) &\equiv \tfrac{1}{2}[I(\phi) + I(-\phi)] = cA_z^2(|\beta M_t|^2 + |M_z|^2), \\ I^-(\phi) &\equiv \tfrac{1}{2}[I(\phi) - I(-\phi)] = 2cA_z^2 \mathrm{Re}(\beta M_t M_z) , \end{aligned} \tag{9}$$

where ϕ is defined as in the preceding paragraph. The interference effects are thereby isolated in the antisymmetric combination $I^-(\phi)$. These combinations have been derived numerically from the data of Fig. 5(a) and the results are shown in Fig. 6. Figure 6(b) corresponds to the data taken with analyzer No. 2, and Fig. 6(a) represents corresponding combinations for the data taken with analyzer No. 1. As mentioned above, mirror symmetry is preserved for analyzer No. 1, so that we expect $I^-(\phi)$ to vanish. This is indeed the case, as indicated by the dashed curve in Fig. 6(a); the rather rapid fluctuations about zero represent the experimental uncertainty. In contrast, the results

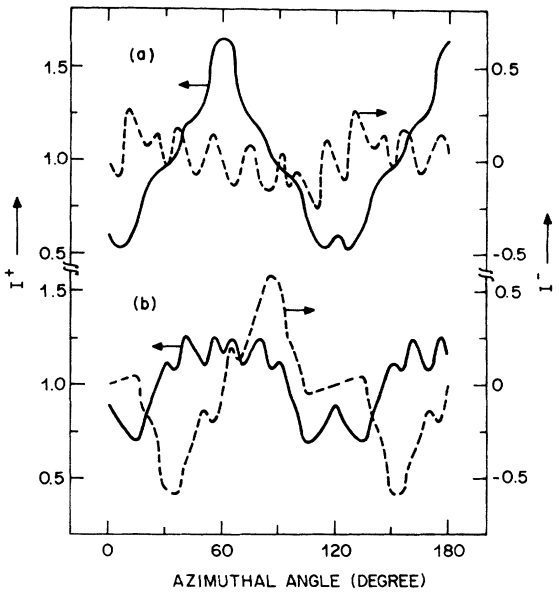

FIG. 6. Azimuthal dependence of the symmetric (full curves) and antisymmetric (dashed curves) combinations of photoemission intensities taken on the In $4d$ levels for $\theta = 60°$ and $\hbar\omega = 33$ eV using (a) analyzer No. 1 and (b) analyzer No. 2.

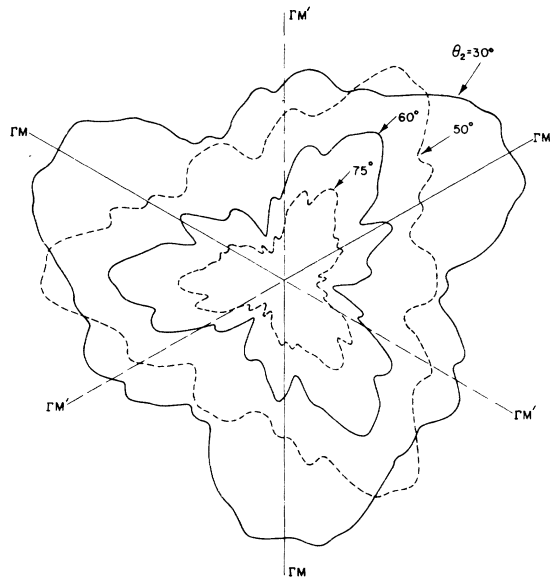

FIG. 7. Azimuthal dependence of the Ga $3d$ photoemission intensity in GaSe for various polar angles, taken with analyzer No. 2 at $\hbar\omega = 33$ eV.

for $\Gamma(\phi)$ in Fig. 6(b) show appreciable amplitude. Note also that mirror symmetry requires that $M_x(\phi)$, and therefore $\Gamma(\phi)$, should vanish whenever $\phi = \frac{1}{6}n\pi$, and this is observed experimentally. In principle, information on the relative values of M_x and M_z can be extracted from the data. We make no attempt to do that here, however, since there are no theoretical predictions with which to compare our conclusions. Instead, we close this part of the discussion with the following purely experimental observation. The information obtained with analyzer No. 1 contains some redundancy since it repeats itself on either side of a crystal mirror plane, and only information on the sum $|\beta M_x|^2 + |M_z|^2$ is obtained. If, in the design of an experimental system, space limitations or other restrictions permit only one analyzer, an out-of-plane analyzer such as analyzer No. 2 could be the better choice in many cases, since it offers more information than the in-plane analyzer.

The dependence of the azimuthal patterns on polar angle of emission θ was investigated. Some results obtained on the Ga $3d$ levels of GaSe using analyzer No. 2 at $\hbar\omega = 33$ eV are shown in Fig. 7. The azimuthal pattern varies quite strongly, becoming progressively more anisotropic with increasing θ. The degree of asymmetry about the ΓM mirror planes also varies with θ. This emerges from detailed analyses of the kind discussed above, but is also evident from visual inspection of Fig. 7. Once again, we have no detailed theoretical interpretation of these results.

With regard to the prospects of photoelectron diffraction as a technique for surface-structure determination, these results on layer compounds (to be thought of as prototype surface systems) are encouraging. We have shown that azimuthal anisotropies are quite strong, and that these anisotropies vary considerably with photoelectron energy, radiation polarization geometry, and polar angle of emission.

V. RESULTS AND DISCUSSION ON CESIATED W(001)

According to a recent model based on LEED experiments,[17] the adsorption of Cs on W (001) involves two sites. At low coverages (less than $\frac{1}{4}$ monolayer), the Cs atoms are thought to occupy the fourfold sites. At higher coverages, it is thought that bridge positions become occupied, ultimately forming a pseudohexagonal close-packed array, with saturation occurring at $\frac{1}{2}$ monolayer.

In Fig. 8, we show spectra obtained with analyzer No. 2 at normal emission for various coverages of Cs. The photon energy was $\hbar\omega = 24$ eV. The Cs coverages are not known with accuracy, but can be estimated from the change in work function. The lowest coverage in Fig. 8, corresponding to curve (a), is estimated to be ~0.04 monolayer. Curves (b)–(d) correspond to progressively higher coverages. For curves (c) and (d), the estimated coverage is in the vicinity of 0.25 monolayer, where the $p(2\times 2)$ LEED pattern and work-function minimum are known to occur.[17] It is observed that the bind-

ing energy of the Cs $5p$ core levels increases with increasing coverage. In curve (a) the $5p_{1/2}$ and $5p_{3/2}$ peaks occur at -13.1 and -11.3 eV, respectively, whereas in curve (d), the corresponding values are -14.2 and -12.3 eV.

We note in passing some features of the data which appear interesting, but were not pursued in detail since they were not germane to the objective of this investigation, namely, the search for anisotropies. The ratio of the intensities under the $5p_{3/2}$ and $5p_{1/2}$ peaks is smaller than that of the eigenvalue multiplicity $(l+1)/l=2$. This has been observed previously by Rowe and Margaritondo[18] who, following Dehmer and Berkowitz,[19] attribute it to intra-atomic effects associated with the photon energy dependence of the relative oscillator strengths. The spectra of Fig. 8, however, show that the $5p_{3/2}/5p_{1/2}$ ratio depends on Cs coverage, and is as low as 0.5 for the highest coverages. This indicates that the nonstatistical ratios are not purely an intra-atomic phenomenon. Another feature is the peak labeled A in the spectra of Fig. 8. The strength of this feature scales closely in proportion to the strength of the Cs $5p$ peaks and maintains a constant energy separation with respect to them. We have no satisfactory explanation for this peak, although it may represent some contaminant, possibly oxygen, from the commercial Cs source.

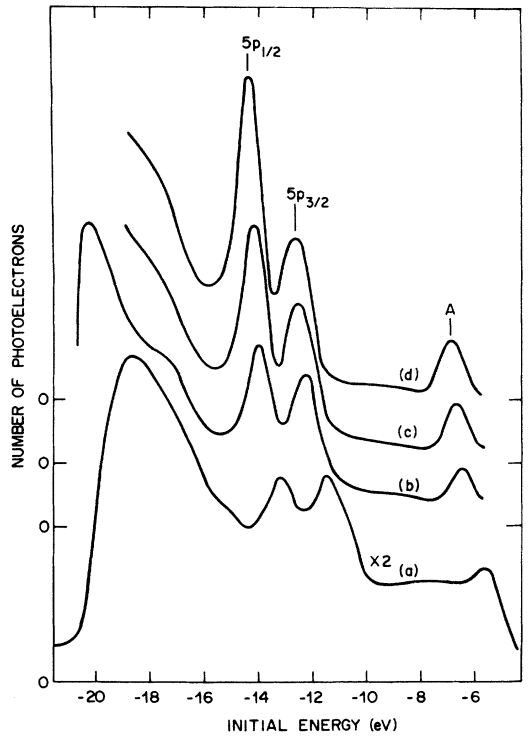

FIG. 8. Photoelectron energy spectra taken at $\hbar\omega=24$ eV for various coverages of Cs on W(001).

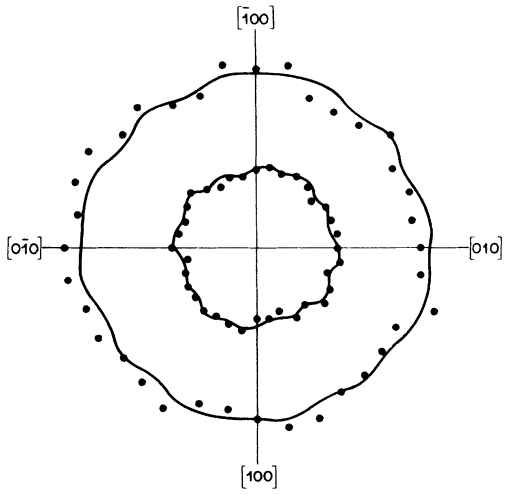

FIG. 9. Azimuthal dependence of the Cs $5p_{3/2}$ photoemission for Cs on W(001) in relatively high-coverage (outer set of data) and low- coverage (inner set of data) situations.

Since A is observed to move with photon energy, it is in no way related to the $\hbar\omega$-independent feature observed by Oswald and Callcott[20] on bulk Cs. Another incidental observation on a high-coverage surface was that the Cs $5p$ peaks displayed a small but significant (~0.4 eV) upwards dispersion in energy as the polar angle was increased from 0° to 70°. This would indicate that the Cs $5p$ levels are not pure core levels, but have some bandlike character.

Returning to our major topic, i.e. anisotropies, we show in Fig. 9 some typical azimuthal patterns for the Cs $5p_{3/2}$ emission. The outer experimental points were obtained at $\theta_2=60°$ and $\hbar\omega=24$ eV on a surface having a relatively high Cs coverage, corresponding to curve (c) of Fig. 8. The inner points were obtained at $\theta_2=60°$ and $\hbar\omega=21$ eV on a surface having the low (~0.04 monolayer) coverage corresponding to curve (a) of Fig. 8. In each case, the smooth curves were drawn through fourfold symmetrized versions of the data. The outer curve shows some ripples, but their amplitude is comparable with the experimental uncertainty, which can be estimated by comparing the fourfold-symmetrized curve with the raw data points. The inner curve also shows ripples, but these appear to be significant. It is noted, again by comparing the smooth curve with the raw points, that some of the bumps repeat reliably every 90°. The peak-to-valley amplitude of these ripples, however, is rather small (~15%). In summary, the emission from the Cs $5p$ core levels on W(001) does display some anisotropy for low coverages, but this anisotropy is near the borderline of experimental significance.

VI. CONCLUDING REMARKS

Concerning the prospects of photoelectron diffraction as a means of determining surface structures, our conclusions are mixed. The strong anisotropies observed in the layer compounds InSe and GaSe offer encouragement. The much weaker anisotropy, if any, observed on the real adsorption system Cs on W(001) is, at first sight, discouraging. Taken at face value, these latter results would indicate that backscattered signal from the substrate, Ψ^1, is too weak to bring about any appreciable interference with the direct signal Ψ^0. We hesitate to draw this as a general conclusion at this stage for the reasons given below.

In testing the feasibility of the photoelectron-diffraction technique, Cs is not the best choice as a prototype adsorbate. The hot-electron attenuation length in bulk Cs is known to be extremely short,[21] being of the order of 1 Å. This means that the backscattered wave, which has to traverse the Cs overlayer at least once, is weakened by attenuation in the Cs itself. It is probably significant that the hints of anisotropy observed, were found at very low Cs coverages. Even here, one is not immune from attenuation if the overlayer growth occurs in islands. Our choice of Cs was determined by the need to find elements with accessible core levels, given the limited photon energy range of the Seya-Namioka monochromator. It would be desirable to perform these experiments at higher photon energies on other adsorbate elements.

ACKNOWLEDGMENTS

We have benefitted, throughout the course of this work, from stimulating discussions with M. M. Traum. We are grateful also to E. M. Rowe, R. A. Otte, and other members of the University of Wisconsin Physical Sciences Laboratory. The Tantalus I storage ring is supported by NSF grant No. DMR-74-15089.

---

*Permanent address: Philips Research Laboratories, Eindhoven, The Netherlands.

†Present address: Dept. of Physics, University of California, Berkeley, California.

[1]K. Siegbahn, U. Gelius, H. Siegbahn, and E. Olson, Phys. Scr. 1, 272 (1970); Phys. Lett. 32A, 221 (1970).

[2]C. S. Fadley and S. A. L. Bergström, Phys. Lett. 35A, 375 (1971).

[3]F. J. Himpsel and W. Steinmann, Phys. Rev. Lett. 35, 1025 (1975).

[4]R. J. Baird, C. S. Fadley, and L. F. Wagner, Phys. Rev. B 15, 666 (1977).

[5]A. Liebsch, Phys. Rev. B 13, 544 (1976); Phys. Rev. Lett. 32, 1203 (1974).

[6]J. B. Pendry, Surf. Sci. 57, 679 (1976).

[7]C. Caroli, D. Lederer-Rozenblatt, B. Roulet, and D. Saint-James, Phys. Rev. B 8, 4552 (1973).

[8]J. W. Gadzuk, Phys. Rev. B 10, 5030 (1974).

[9]N. V. Smith, P. K. Larsen, and M. M. Traum, Rev. Sci. Instrum. 48, 454 (1977).

[10]N. V. Smith and M. M. Traum, Phys. Rev. B 11, 2087 (1975).

[11]P. K. Larsen, S. Chiang, and N. V. Smith, Phys. Rev. B 15, 3200 (1977).

[12]P. K. Larsen, M. Schlüter, and N. V. Smith, Solid State Commun. 21, 775 (1977).

[13]B. Feuerbacher and M. R. Adriaens, Surf. Sci. 45, 553 (1974); R. F. Willis, B. Feuerbacher, and B. Fitton, Solid State Commun. 18, 1315 (1976).

[14]G. J. Lapeyre, R. J. Smith, and J. Anderson, J. Vac. Sci. Technol. 14, 386 (1977).

[15]M. M. Traum (unpublished); and (private communication).

[16]J. G. Endriz, Phys. Rev. B 7, 3464 (1973); S. P. Weeks and E. W. Plummer, Solid State Commun. 21, 695 (1977).

[17]V. B. Voronin, A. G. Naumovets, and A. G. Fedorus, Pis'ma Zh. Eskp. Teor. Fiz. 15, 523 (1972) [JETP Lett. 15, 370 (1972)]; C. A. Papageorgopoulos and J. M. Chen, J. Phys. C 6, L279 (1973). The earlier "duolayer" model appears to have been based on an incorrect assignment of the low-coverage $c(2\times 2)$ structure; A. U. MacRae, K. Muller, J. J. Lander, J. Morrison, and J. C. Phillips, Phys. Rev. Lett. 22, 1048 (1969).

[18]J. E. Rowe and G. Margaritondo, Phys. Lett. 57A, 314 (1976).

[19]J. L. Dehmer and J. Berkowitz, Phys. Rev. A 10, 484 (1974).

[20]R. G. Oswald and T. A. Callcott, Phys. Rev. B 4, 4122 (1971).

[21]N. V. Smith and G. B. Fisher, Phys. Rev. B 3, 3662 (1971).